






# Düzce University Journal of Science & Technology

Research Article

## Investigation of Cement, Mineral and Chemical Additive Interactions in Micro Scales

 Murat GÖKÇE <sup>a</sup>,  Osman ŞİMŞEK <sup>b</sup>,  Kenan TOKLU <sup>c,\*</sup>

<sup>a</sup>, Department of Architecture, Faculty of Architecture, Amasya University, Amasya, TURKEY

<sup>b</sup> Department of Civil Engineering, Faculty of Technology, Gazi University, Ankara, TURKEY

<sup>c</sup> Department of Civil Engineering, Çorlu Faculty of Engineering, Tekirdağ Namık Kemal University, Tekirdağ, TURKEY

\* Corresponding author's e-mail address: ktoklu@nku.edu.tr

DOI: 10.29130/dubited.944934

### ABSTRACT

Self-compacting concretes (SCC), a new type of concrete, were realized with the development of polycarboxylate-based chemical additives. The interaction of these additives with the powder materials in the nano and micro scales affects the fresh and hardened properties of concrete in meso and macro scales. To change and improve the macro-dimensional properties of concrete, it is necessary to better analyze the nano-micro-dimensional interaction. The aim of this study is to examine the interactions of cement, mineral and chemical additives in micro scale. For this purpose, the zeta potential values of the mixtures consisting of cement, water, calcite and blast furnace slag prepared by using a polycarboxylate based plasticizer additive were analyzed. In addition, SEM analyzes of hardened samples were made on the 28<sup>th</sup> days.

**Keywords:** Zeta potential, Polycarboxylate-based chemical additive, SEM image

## Mikro Boyutlarda Çimento, Mineral ve Kimyasal Katkı Etkileşimlerinin İncelenmesi

### ÖZ

Polikarboksilat esaslı kimyasal katkıların geliştirilmesi ile yeni bir beton türü olan kendiliğinden yerleşen betonlar (KYB) hayata geçirilmiştir. Bu katkı maddelerinin nano ve mikro boyutlardaki toz malzemelerle etkileşimi, betonun taze ve sertleşmiş özelliklerini mezo ve makro boyutlarda etkilemektedir. Betonun makro boyutlu özelliklerini değiştirmek ve iyileştirmek için nano-mikro boyutlu etkileşimini daha iyi analiz etmek gerekmektedir. Bu çalışmanın amacı çimento, mineral ve kimyasal katkı maddelerinin etkileşimlerini mikro ölçekte incelemektir. Bu amaçla polikarboksilat esaslı plastikleştirici katkı kullanılarak hazırlanan çimento, su, kalsit ve yüksek fırın cürufundan oluşan karışımların zeta potansiyel değerleri analiz edilmiştir. Ayrıca 28. günde sertleşmiş numunelerin SEM analizleri yapılmıştır.

**Anahtar Kelimeler:** Zeta potansiyeli, Polikarboksilat bazlı kimyasal katkı, SEM görüntüsü

Received: 30/05/2021, Revised: 20/06/2021, Accepted: 26/06/2021

\*This study is produced from Doctoral Thesis titled "Investigation of the interaction of paste phase with chemical admixtures in self-consolidating concrete".

## INTRODUCTION

Researchers have produced self-compacting concrete (SCC), which is one of the latest generation concrete types, having high flow-passing capability and stability properties over the last decades [1]. Due to these properties, SCC is a concrete that can be placed on the molds with its own weight without vibration or too little vibration [2]. In addition, it is a concrete type that is cohesive enough to be processed by eliminating the negative properties of its fresh state such as segregation and bleeding [2]. Thus, high strength concrete having low energy consumption, low labor costs and low porosity can be easily produced [3]. In order to produce the freshly SCC having the desired properties, chemical additives such as a particularly effective superplasticizer and a higher proportion of ultra-thin materials should be added to the mixture [4,5].

With the help of super plasticizers or high water reducers, the workability of the concrete increases with the good dispersion of the cement particles in the concrete mixture, and thus the amount of mixing water decreases [6]. However, the interaction of the cement and superplasticizer is not fully understood and research on this subject is ongoing [7]. There are many ways for determining the optimum dosage of the superplasticizers in the mixture, such as slump test [8,9], the flow table test [9,10] and Marsh cone test [9,11] in terms of rheological perspective [9]. However, these tests only give information about the flow of cement paste and do not give information about the dispersion of cement grains, which is the main effect of superplasticizer in cement paste [9]. Different methods are applied to examine the interaction between colloidal particles and superplasticizers [12]. One of them is the measurement of the zeta potential of cement-water suspensions [12]. The zeta potential, which is the measurability of an electrical interface, is used in electrical double layer theory [13] (Figure 1). The zeta potential is affected by the surface structure of the solid particles and the content of the liquid [14-20].

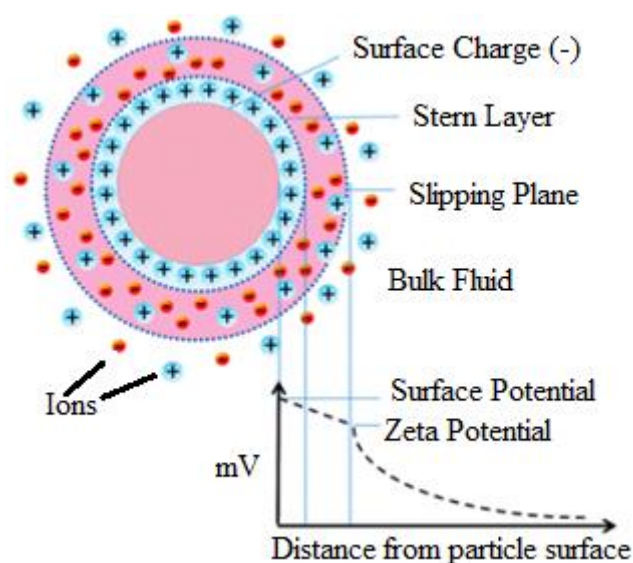


*Figure 1. Configuration of double layer [21]*

In the study conducted by Ersoy et al. [22], time dependent zeta potentials of the pure clinker phase of normal portland cement were measured. As a result, they found that the C3S phase showed positive zeta potential. They also emphasized that the ambient pH does not affect the zeta potential of the C3S phase much, but the +2 valence  $\text{Ca}^{+2}$  ions are the main parameter in the zeta potential of the C3S phase. Lastly, the authors said that there was a weak relationship between hydration temperature data and time-dependent zeta potential data.

Yıldız et al. [23] examined the mineralogical, molecular, zeta potential and simultaneous thermal compatibility of usage of pumice and zeolite in high strength concrete. According to the analysis results, it is stated that CEM I 42.5 R is suitable for surface charges of pumice and zeolite, but CEM I 42.5 R and pumice are more electrokinetically compatible.

Srinivasan et al. [9] investigated that the superplasticizers were absorbed by cement particles and the zeta potential formed between the interfaces of these particles was measured using electroacoustic technique. The study investigated both the zeta potential magnitude for ordinary Portland cement and Portland pozzolanic cement pastes and also the effects of different superplasticizers on these cement types. When the results were analyzed, Portland pozzolanic cement pastes showed a better distribution than ordinary Portland cement pastes. The article also tried to reveal the importance of the interaction of three different superplasticizers with cement. In general, it was concluded that one of the best ways to understand the absorptive and dispersing effect of superplasticizers in cement paste is by measuring the zeta potential of cement suspensions.

In another study [24], the general method, which takes into account the experimentally achievable total surface conductivity, has been introduced in the analysis of ESA data obtained from partially concentrated suspensions. When the zeta potentials obtained and the zeta potentials without taking into account contribution of the stagnant layer to surface conductivity were compared, it was found that the zeta potential obtained is unambiguously higher than the other. Also in this study, the mobility of potassium and magnesium ions in stagnant layer in terms of hydrodynamic was analyzed. It has been concluded that while the level of magnesium mobility is considerably decreased, the ionic mobility of potassium has the same magnitude as in bulk solution [24].

The aim of this study is to examine the interactions of cement, mineral and chemical additives in micro scale. For this purpose, the zeta potential values of the mixtures consisting of cement, water, calcite and blast furnace slag prepared by using a polycarboxylate based plasticizer additive were analyzed. In addition, SEM analyzes of hardened cement pastes were made on the 28<sup>th</sup> days.

## **II. MATERIAL AND METHOD**

### **A. MATERIAL**

#### **A. 1. Chemical Additive**

Polycarboxylate based chemical additive was used in this study. Table 1 shows the physical properties of the chemical additive.

*Table 1. Physical properties of the chemical additive*

<b>Features</b>	<b>Values</b>
Density (g/cm <sup>3</sup> )	1.06
pH	5.6
Solid matter (%)	25

#### **A. 2. Blast Furnace Slag (BFS)**

The density and specific surface area of the BFS obtained from Kardemir Karabuk Iron and Steel Factory is 3 g/cm<sup>3</sup> and the is 3785 cm<sup>2</sup>/g, respectively. Table 2 shows the chemical analysis of BFS.

**Table 2.** Chemical analysis of BFS

Oxide	SiO <sub>2</sub>	CaO	Al <sub>2</sub> O <sub>3</sub>	MgO	MnO	SO <sub>3</sub>	Fe <sub>2</sub> O <sub>3</sub>	K <sub>2</sub> O	Na <sub>2</sub> O	TiO <sub>2</sub>
Content (%)	38.5	36.31	9.98	7.8	2.92	0.63	0.66	1.38	0.23	1.31

### A. 3. Calcite

In this study, calcite obtained from the Sivrihisar region and passed under a 75 micron sieve used. The density and specific surface area of calcite are 2.72 g/cm<sup>3</sup> and 4160 cm<sup>2</sup>/g, respectively. Table 3 shows the chemical analysis of calcite.

**Table 3.** Chemical analysis of calcite

Oxide	SiO <sub>2</sub>	CaO	Al <sub>2</sub> O <sub>3</sub>	MgO	SO <sub>3</sub>	Na <sub>2</sub> O	K <sub>2</sub> O
Content (%)	0.01	53.94	0.07	1.93	0.01	0.06	0.13

### A. 4. Cement

CEM I 42.5 R cement was used in the study. Table 4 shows the physical and chemical properties of the cement.

**Table 4.** Physical and chemical properties of cement

Physical Properties								
Density (g/cm <sup>3</sup> )	Blaine (cm <sup>2</sup> /g)	2 days strength (MPa)	7 days strength (MPa)	28 days strength (MPa)	Initial setting (min)	Final setting (min)	Volume expansion (mm)	LOI* (%)
3.1	3300	27.3	40.8	51.7	162	282	1	2.5
Chemical Properties (%)								
SO <sub>3</sub>	Cl	SiO <sub>2</sub>	Al <sub>2</sub> O <sub>3</sub>	Fe <sub>2</sub> O <sub>3</sub>	CaO	MgO	Na <sub>2</sub> O	K <sub>2</sub> O
2.81	0.01	20.04	5.27	3.38	62.23	1.89	0.04	0.78

\*Loss on ignition

## B. METHOD

Samples were prepared to understand the starting interaction of polycarboxylate based chemical additives with powder materials in the concrete in micro scales. Samples prepared for this purpose were produced as follows; the amounts of the binder, water, chemical additives were kept constant in all cement paste prepared and reference cement paste. Then, BFS was added as a replacement material to cement at the rates of 10%, 20%, 30% and 40% of cement weight and calcite was added as an additional material to mixture at the rates of 10%, 15%, 20% and 25% of cement weight in mixture. Mixture quantities and rates are given in Table 5.

**Table 5. Mixing amounts and ratios for cement pastes**

Mixture	Materials (g)					Abbreviation
	Cement	Water	Calcite	BFS	Polycarboxylate Based Chemical Additive	
R	1000	330	0	0	10	R=Reference
RCa10	1000	330	100	0	10	RCa10 = R + 10 wt% Ca
RCa15	1000	330	150	0	10	RCa15 = R + 15 wt% Ca
RCa20	1000	330	200	0	10	RCa20 = R + 20 wt% Ca
RCa25	1000	330	250	0	10	RCa25 = R + 25 wt% Ca
C90BFS10	900	330	0	100	10	C90BFS10=90% Cement + 10 wt% BFS
C80BFS20	800	330	0	200	10	C80BFS20=80% Cement + 20 wt% BFS
C70BFS30	700	330	0	300	10	C70BFS30=70% Cement + 30 wt% BFS
C60BFS40	600	330	0	400	10	C60BFS40=60% Cement + 40 wt% BFS
C90BFS10Ca10	900	330	100	100	10	C90BFS10Ca10 =90% Cement + 10 wt% BFS +10 wt% Ca
C90BFS10Ca15	900	330	150	100	10	C90BFS10Ca15 =90% Cement + 10 wt% BFS +15 wt% Ca
C90BFS10Ca20	900	330	200	100	10	C90BFS10Ca20 =90% Cement + 10 wt% BFS +20 wt% Ca
C90BFS10Ca25	900	330	250	100	10	C90BFS10Ca25 =90% Cement + 10 wt% BFS +25 wt% Ca
C80BFS20Ca10	800	330	100	200	10	C80BFS20Ca10 =80% Cement + 20 wt% BFS +10 wt% Ca
C80BFS20Ca15	800	330	150	200	10	C80BFS20Ca15 =80% Cement + 20 wt% BFS +15 wt% Ca
C80BFS20Ca20	800	330	200	200	10	C80BFS20Ca20 =80% Cement + 20 wt% BFS +20 wt% Ca
C80BFS20Ca25	800	330	250	200	10	C80BFS20Ca25 =80% Cement + 20 wt% BFS +25 wt% Ca
C70BFS30Ca10	700	330	100	300	10	C70BFS30Ca10 =70% Cement + 30 wt% BFS +10 wt% Ca
C70BFS30Ca15	700	330	150	300	10	C70BFS30Ca15 =70% Cement + 30 wt% BFS +15 wt% Ca
C70BFS30Ca20	700	330	200	300	10	C70BFS30Ca20 =70% Cement + 30 wt% BFS +20 wt% Ca
C70BFS30Ca25	700	330	250	300	10	C70BFS30Ca25 =70% Cement + 30 wt% BFS +25 wt% Ca
C60BFS40Ca10	600	330	100	400	10	C60BFS40Ca10 =60% Cement + 40 wt% BFS +10 wt% Ca
C60BFS40Ca15	600	330	150	400	10	C60BFS40Ca15 =60% Cement + 40 wt% BFS +15 wt% Ca
C60BFS40Ca20	600	330	200	400	10	C60BFS40Ca20 =60% Cement + 40 wt% BFS +20 wt% Ca
C60BFS40Ca25	600	330	250	400	10	C60BFS40Ca25 =60% Cement + 40 wt% BFS +25 wt% Ca

-BFS was used a partial cement replacement in the mixtures, Ca was added to cement as an additional material.

## B. 1. Experiments For Samples Having Micro Size

The zeta potential is measured by ultrasonic sound waves, the vibrations emitted by the particles according to the surface charge potential value, as a result of the electric field applied to the mixture consisting of the pastes placed in the cell of the test device (Figure 2). The speed and dynamic mobility of the particles were calculated from the sound waves emitted by vibrations. As a result of the experiment, zeta potential values were obtained as Mv unit.

While preparing the pastes, mixing was done according to TS EN 197-1 [25]. The prepared pastes were placed in the zeta potential measuring device and the experiment was continued for 15 minutes and a measurement result was taken every 30 seconds. In the zeta potential device, it is mixed with a mixer at a constant speed (60 rpm) so that pastes remain homogeneous during the experiment. The data obtained after 15 minutes (zeta potential, ESA) were recorded by taking the average. Samples taken pastes prepared for zeta potential measurements placed to molds having 5 mm diameter and 3 mm height for SEM analysis. SEM analysis of hardened paste samples were performed at days 1, 7 and 28. While SEM analysis was performed on 1-day samples without curing, it was performed on 7 and 28 day samples subjected to water curing at  $20 \pm 1$  ° C. The zeta potential for each prepared paste and SEM analysis for the hardened samples were made in this study.

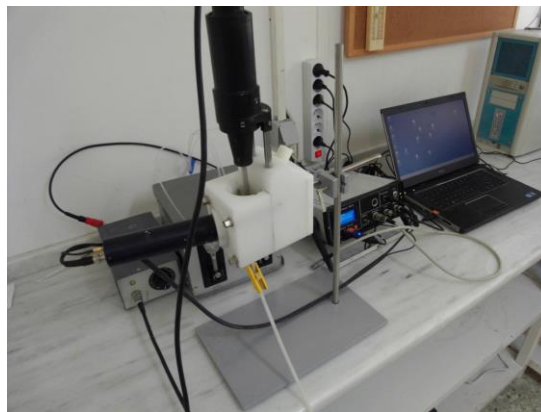


*Figure 2. Zeta potential measurement test device*

## III. RESEARCH FINDINGS

Large particles of BFS have more smoother edge lines and smoother surface texture than smaller particles as seen from Figure 3.

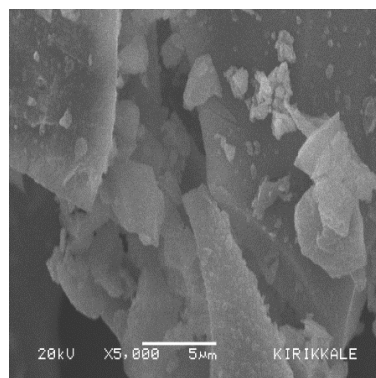


*Figure 3. SEM micro image of BFS*

In the SEM analysis given in Figure 4, it is observed that the calcite sample has more irregular geometric shapes, more rough surface texture compared to the BFS.

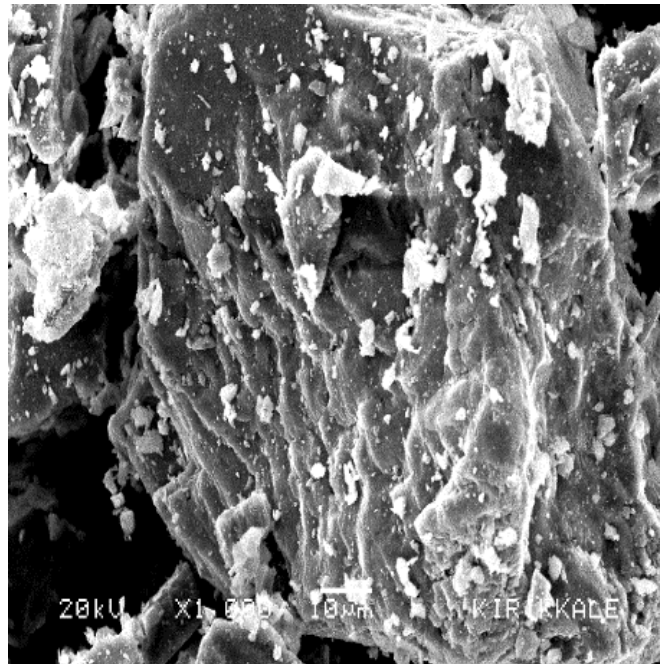


*Figure 4. SEM micro image of calcite [26]*

As seen in Table 6, the highest zeta potential was found as 94.6 mV in the cement paste mixture, which is C60BFS40Ca10 (C:cement, BFS: blast furnace slag, Ca: calcite). The lowest zeta potential was determined as 52.8 mV in the reference sample. In addition, it is seen in Table 6 that an increase in zeta potential values was generally occurred by adding calcite to cement for reference samples. The addition of 20% calcite to the reference sample provided the greatest increase in zeta potential value compared to other reference samples. BFS substitutions increased zeta potential values compared to the reference sample. The zeta potential value of the paste with 20% BFS substitution was higher than those produced at 10%, 30% and 40% BFS substitution rates. With the addition of 10%, 15%, 20% and 25% calcite to C90BFS10 paste, calcite addition rates increased but zeta potential values decreased. In the same way, with the addition of 10%, 15%, 20% and 25% calcite to C80BFS20 paste, calcite addition rates increased but zeta potential values decreased. While the zeta potential values decreased with the increase of calcite addition rates in the paste mixes that added 10%, 20% and 25% calcite to the C70BFS30 paste, the zeta potential increased in the 15% calcite addition mixture, which is C70BFS30Ca15. Also, while the zeta potential values decreased in the paste mixes where 15% calcite was added to the C60BFS40 paste, the zeta potential values increased in the mixture of C60BFS40Ca10, C60BFS40Ca20 and C60BFS40Ca25.

The reason for the serious differences of the zeta potentials obtained is that the grain sizes of the powder materials (cement, BFS and Ca) used in the paste phase are different from each other and large according to this test method.

**Table 6.** Results of zeta potential for all samples

Mixture	Zeta Potential (mV)	ESA (mPa*M/V)	Abbreviation
R	52.8	1.24	R=Reference
RCa10	53.6	1.20	RCa10 = R + 10 wt% Ca
RCa15	56.5	1.24	RCa15 = R + 15 wt% Ca
RCa20	85.2	1.83	RCa20 = R + 20 wt% Ca
RCa25	82.0	1.72	RCa25 = R + 25 wt% Ca
C90BFS10	61.0	1.42	C90BFS10 =90% Cement + 10 wt% BFS
C80BFS20	78.5	1.4	C80BFS20 =80% Cement + 20 wt% BFS
C70BFS30	60.9	1.39	C70BFS30=70% Cement + 30 wt% BFS
C60BFS40	56.4	1.29	C60BFS40=60% Cement + 40 wt% BFS
C90BFS10Ca10	81.7	1.79	C90BFS10Ca10 =90% Cement + 10 wt% BFS +10 wt% Ca
C90BFS10Ca15	79.5	1.73	C90BFS10Ca15 =90% Cement + 10 wt% BFS +15 wt% Ca
C90BFS10Ca20	75.6	1.61	C90BFS10Ca20 =90% Cement + 10 wt% BFS +20 wt% Ca
C90BFS10Ca25	70.7	1.57	C90BFS10Ca25 =90% Cement + 10 wt% BFS +25 wt% Ca
C80BFS20Ca10	87.8	1.87	C80BFS20Ca10 =80% Cement + 20 wt% BFS +10 wt% Ca
C80BFS20Ca15	83.5	1.77	C80BFS20Ca15 =80% Cement + 20 wt% BFS +15 wt% Ca
C80BFS20Ca20	81.7	1.81	C80BFS20Ca20 =80% Cement + 20 wt% BFS +20 wt% Ca
C80BFS20Ca25	79.5	1.73	C80BFS20Ca25 =80% Cement + 20 wt% BFS +25 wt% Ca
C70BFS30Ca10	85.9	1.83	C70BFS30Ca10 =70% Cement + 30 wt% BFS +10 wt% Ca
C70BFS30Ca15	92.5	1.93	C70BFS30Ca15 =70% Cement + 30 wt% BFS +15 wt% Ca
C70BFS30Ca20	79.9	1.76	C70BFS30Ca20 =70% Cement + 30 wt% BFS +20 wt% Ca
C70BFS30Ca25	77.9	1.69	C70BFS30Ca25 =70% Cement + 30 wt% BFS +25 wt% Ca
C60BFS40Ca10	94.6	1.96	C60BFS40Ca10 =60% Cement + 40 wt% BFS +10 wt% Ca
C60BFS40Ca15	76.3	1.64	C60BFS40Ca15 =60% Cement + 40 wt% BFS +15 wt% Ca
C60BFS40Ca20	84.5	1.75	C60BFS40Ca20 =60% Cement + 40 wt% BFS +20 wt% Ca
C60BFS40Ca25	87.0	1.82	C60BFS40Ca25 =60% Cement + 40 wt% BFS +25 wt% Ca

-BFS was used a partial cement replacement in the mixtures, Ca was added to cement as an additional material.

Figure 5 shows the SEM image of the 28-day reference paste and also the EDS analysis (Figure 6) of the region indicated by the red line. According to the results of EDS and SEM analyzes, it is seen that calcium silicate hydrates are in the majority in this region.



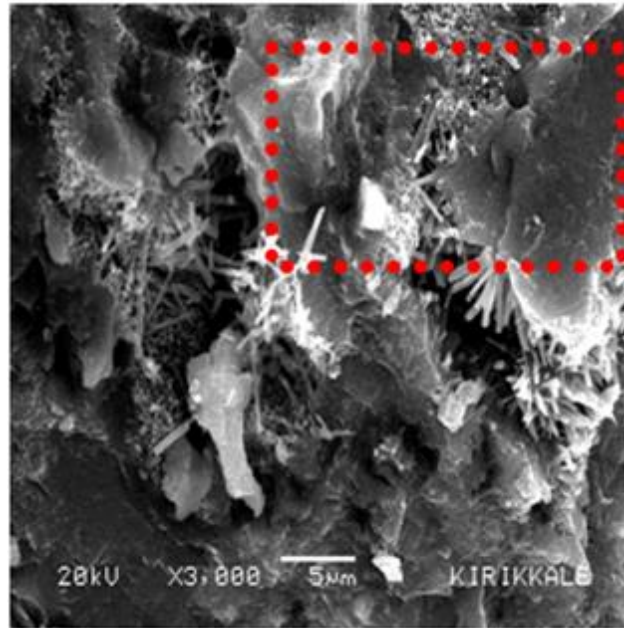


Figure 5. SEM image of the reference cement paste on the 28<sup>th</sup> day

Component	Type	Mole Conc.	Conc.		
C O2	Calc	0,000	0,000	wt. %	
MgO	Calc	3,099	2,128	wt. %	
Al2O3	Calc	1,289	2,240	wt. %	
SiO2	Calc	32,884	33,665	wt. %	
SO3	Calc	1,911	2,607	wt. %	
Cl2O	Calc	0,211	0,312	wt. %	
K2O	Calc	0,123	0,197	wt. %	
CaO	Calc	59,884	57,218	wt. %	
Fe2O3	Calc	0,600	1,634	wt. %	
		100,000	100,000	wt. %	Total
El.	Line	Intensity (c/s)	Error 2-sig	Conc	
C	Ka	8,08	1,271	0,000	wt. %
O	Ka	42,65	2,921	38,296	wt. %
Mg	Ka	11,63	1,525	1,284	wt. %
Al	Ka	12,74	1,596	1,186	wt. %
Si	Ka	189,83	6,162	15,736	wt. %
S	Ka	11,99	1,548	1,044	wt. %
Cl	Ka	2,93	0,765	0,254	wt. %
K	Ka	1,90	0,617	0,163	wt. %
Ca	Ka	414,14	9,101	40,894	wt. %
Fe	Ka	5,13	1,013	1,143	wt. %
				100,000	wt. % Total
kV		20,0			
Takeoff Angle		35,0°			
Elapsed Livetime		20,0			

Figure 6. EDS analysis of the region indicated by the red line on the SEM image for the reference cement paste on the 28<sup>th</sup> day

In the 28-day SEM analysis of hardened cement paste (Figure 7), RCa25, the presence of ettringite in the region marked with the red line was determined according to the EDS (Figure 8) result.

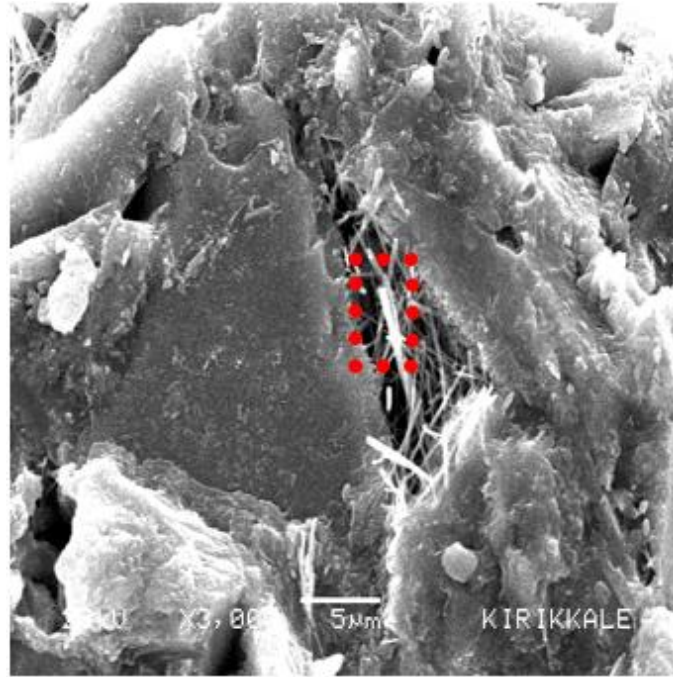


Figure 7. SEM image of the RCa25 paste on the 28<sup>th</sup> day

Component	Type	Mole Conc.	Conc.	
C O2	Calc	0,000	0,000	wt.%
MgO	Calc	1,402	0,916	wt.%
Al2O3	Calc	2,639	4,361	wt.%
SiO2	Calc	17,848	17,379	wt.%
P2O5	Calc	2,897	6,665	wt.%
SO3	Calc	2,888	3,747	wt.%
Cl2O	Calc	0,112	0,158	wt.%
CaO	Calc	71,085	64,604	wt.%
MnO2	Calc	0,636	0,896	wt.%
Fe2O3	Calc	0,492	1,273	wt.%
		100,000	100,000	wt.%
				Total
El.	Line	Intensity (c/s)	Error 2-sig	Conc
C	Ka	0,00	0,000	0,000 wt.%
O	Ka	8,53	1,306	36,847 wt.%
Mg	Ka	1,73	0,588	0,552 wt.%
Al	Ka	8,66	1,316	2,308 wt.%
Si	Ka	34,03	2,609	8,124 wt.%
P	Ka	11,54	1,519	2,909 wt.%
S	Ka	6,27	1,120	1,501 wt.%
Cl	Ka	0,54	0,327	0,129 wt.%
Ca	Ka	164,68	5,739	46,173 wt.%
Mn	Ka	1,00	0,447	0,566 wt.%
Fe	Ka	1,41	0,531	0,891 wt.%
				100,000 wt.%
				Total
kV		20,0		
Takeoff Angle		35,0°		
Elapsed Livetime		20,0		

Figure 8. EDS analysis of the region indicated by the red line on the SEM image for the RCa25 paste on the 28<sup>th</sup> day.

The presence of calcium aluminate hydrate in the region marked with the red line on the lower left of the SEM image (Figure 9) for the C60BFS40Ca25 paste on the 28<sup>th</sup> day was determined according to the EDS result (Figure 10 (a)). In addition, the presence of calcium silicate hydrate in the region marked with the red line on the upper of the SEM image for the C60BFS40Ca25 paste on the 28<sup>th</sup> day

was determined according to the EDS result (Figure 10 (b)). Lastly, the presence of ettringite in the region marked with the red line on the middle of the SEM image (Figure 11) for the C60BFS40Ca25 paste on the 28<sup>th</sup> day was determined according to the EDS result (Figure 12).

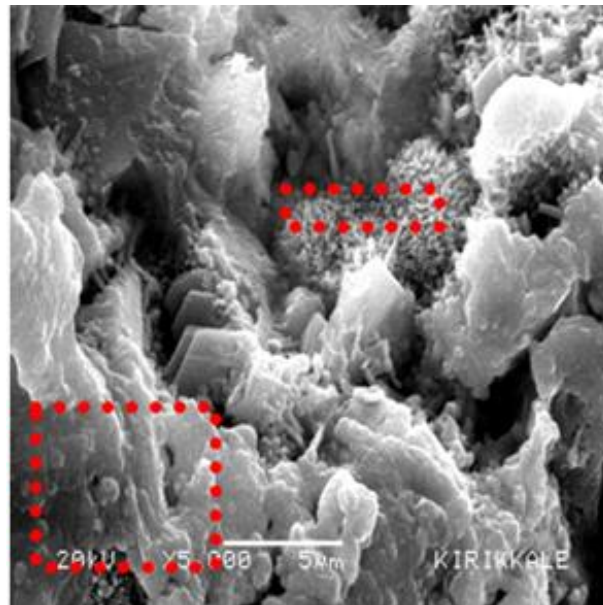


Figure 9. SEM image of the C60BFS40Ca25 paste on the 28<sup>th</sup> day

Component	Type	Mole Conc.	Conc.	
C O2	Calc	0,000	0,000	wt. %
MgO	Calc	1,729	1,116	wt. %
Al2O3	Calc	7,943	12,975	wt. %
SiO2	Calc	23,570	22,688	wt. %
SO3	Calc	1,548	1,986	wt. %
Cl2O	Calc	1,138	1,584	wt. %
K2O	Calc	0,316	0,476	wt. %
CaO	Calc	62,616	56,256	wt. %
Fe2O3	Calc	1,141	2,919	wt. %
		100,000	100,000	Total

El.	Line	Intensity (c/s)	Error 2-sig	Conc	
C	Ka	29,17	2,415	0,000	wt. %
O	Ka	56,03	3,348	37,123	wt. %
Mg	Ka	5,93	1,089	0,673	wt. %
Al	Ka	71,90	3,792	6,867	wt. %
Si	Ka	116,07	4,818	10,605	wt. %
S	Ka	8,94	1,337	0,795	wt. %
Cl	Ka	14,55	1,706	1,292	wt. %
K	Ka	4,45	0,944	0,395	wt. %
Ca	Ka	398,91	8,932	40,206	wt. %
Fe	Ka	8,93	1,336	2,042	wt. %
				100,000	Total
kV		20,0			
Takeoff Angle		35,0°			
Elapsed Livetime		20,0			

Component	Type	Mole Conc.	Conc.	
C O2	Calc	0,000	0,000	wt. %
MgO	Calc	2,899	1,970	wt. %
Al2O3	Calc	2,289	3,935	wt. %
SiO2	Calc	29,813	30,201	wt. %
SO3	Calc	1,465	1,977	wt. %
Cl2O	Calc	0,397	0,581	wt. %
K2O	Calc	0,571	0,907	wt. %
CaO	Calc	61,838	58,467	wt. %
Fe2O3	Calc	0,728	1,961	wt. %
		100,000	100,000	Total

El.	Line	Intensity (c/s)	Error 2-sig	Conc	
C	Ka	35,29	2,657	0,000	wt. %
O	Ka	24,51	2,214	37,434	wt. %
Mg	Ka	7,34	1,211	1,188	wt. %
Al	Ka	15,26	1,747	2,083	wt. %
Si	Ka	114,93	4,794	14,117	wt. %
S	Ka	6,27	1,120	0,792	wt. %
Cl	Ka	3,77	0,868	0,474	wt. %
K	Ka	6,03	1,098	0,753	wt. %
Ca	Ka	288,38	7,594	41,787	wt. %
Fe	Ka	4,22	0,918	1,372	wt. %
				100,000	Total
kV		20,0			
Takeoff Angle		35,0°			
Elapsed Livetime		20,0			

(a)

(b)

Figure 10. (a) EDS analysis of the region indicated by the red line on the lower left of the SEM image for the C60BFS40Ca25 paste on the 28<sup>th</sup> day. (b) EDS analysis of the region indicated by the red line on the upper of the SEM image for the C60BFS40Ca25 paste on the 28<sup>th</sup> day.

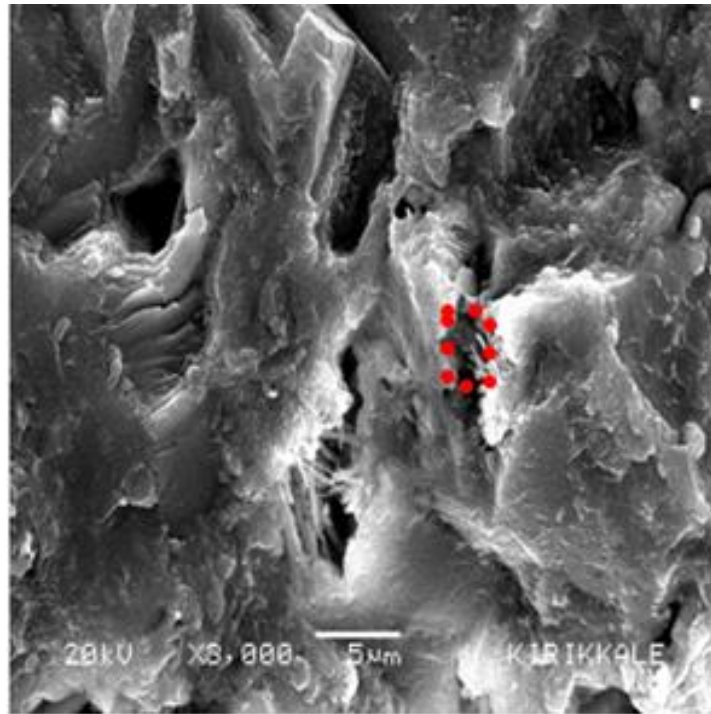


Figure 11. SEM image of the C60BFS40Ca25 paste on the 28<sup>th</sup> day

Component	Type	Mole Conc.	Conc.		
C O2	Calc	0,000	0,000	wt. %	
MgO	Calc	0,306	0,207	wt. %	
Al2O3	Calc	2,165	3,705	wt. %	
SiO2	Calc	6,505	6,561	wt. %	
SO3	Calc	5,267	7,079	wt. %	
Cl2O	Calc	0,137	0,200	wt. %	
K2O	Calc	0,354	0,559	wt. %	
CaO	Calc	84,450	79,499	wt. %	
Fe2O3	Calc	0,817	2,191	wt. %	
		100,000	100,000	wt. %	
				Total	
Elt.	Line	Intensity (cps)	Error 2-sig	Conc.	
C	Ka	9,21	1,357	0,000	wt. %
O	Ka	7,75	1,245	33,035	wt. %
Mg	Ka	0,42	0,289	0,125	wt. %
Al	Ka	7,94	1,260	1,961	wt. %
Si	Ka	14,08	1,678	3,067	wt. %
S	Ka	14,19	1,685	2,835	wt. %
Cl	Ka	0,80	0,399	0,163	wt. %
K	Ka	2,36	0,687	0,464	wt. %
Ca	Ka	227,64	6,747	56,818	wt. %
Fe	Ka	2,66	0,730	1,533	wt. %
				100,000	wt. %
					Total
kV		20,0			
Takeoff Angle		35,0°			
Elapsed Livetime		20,0			

Figure 12. EDS analysis of the region indicated by the red line on the middle of the SEM image for the C60BFS40Ca25 paste on the 28<sup>th</sup> day.

## **IV. CONCLUSION**

The highest zeta potential value was obtained for C60BFS40Ca10 paste (94.6 mV). The lowest zeta potential was 52.8 mV for the reference sample. It has been determined that with the increase of calcite additions to the reference samples, it increases the zeta potential results.

The reason for the serious differences of the zeta potentials of the paste mixes is that the grain sizes of the powder materials (cement, BFS, Ca) used in the paste phase are very large compared to this test method.

In order for the measurement results with zeta potential to be more consistent, it will be necessary to work with much finer powder materials (cement, mineral additives, calcite). The specific surface area of all powder materials greater than 5000 cm<sup>2</sup>/gr can provide more consistent zeta potential results.

In the SEM analysis, it was observed that the calcium hydroxide rate in the environment decreased and C-S-H gels increased after 28 days with the increase of BFS rate. So, as new calcium silica hydrate gels are generated as a result of reactions of BFSs with calcium hydroxides, it has been observed that the amount of calcium hydroxide decreases in hardened pastes. In the SEM analysis, with the increase of the calcite addition rate, the volume of powder material increased and the micro voids decreased.

## **V. REFERENCES**

- [1] O.R. Khaleel, S.A. Al-Mishhadani, H.A. Razak, "The effect of coarse aggregate on fresh and hardened properties of self-compacting concrete (SCC)," *Procedia Engineering*, vol. 14, pp. 805-813, 2011.
- [2] H.A. Mohamed, "Effect of fly ash and silica fume on compressive strength of self-compacting concrete under different curing conditions," *Ain Shams Engineering Journal*, vol.2, no.2, pp. 79-86, 2011.
- [3] C. Karakurt, A.O. Çelik, V. Kiriççi, E. Özyaşar, C. Yılmaz, "Kendiliğinden yerleşen beton davranışının hesaplamalı akışkanlar dinamiği ile benzetimi," *Dokuz Eylül Üniversitesi-Mühendislik Fakültesi Fen ve Mühendislik Dergisi*, vol. 20, no. 59, pp. 449-460, 2018.
- [4] L. Iures, C. Bob, "The Future Concrete: Self-Compacting Concrete," *Buletinul Institutului Politehnic din Iasi. Sectia Constructii, Arhitectura*, vol. 56, no. 2, pp. 93, 2010.
- [5] P.W. Zakka, O.F. Job, N.A. Anigbogu, "Ecological selfcompacting concrete using Gum Arabic as a plasticizer," *West Africa Built Environment Research Conference*, Ghana, pp. 10, 2015.
- [6] Y. Houst, P. Bowen, A. Siebold, "Some basic aspects of the interaction between cement and superplasticizers," *Innovations and Developments in Concrete Materials and Construction*, vol. 12, pp. 225-234, 2002.
- [7] J., Plank, C. Hirsch, "Impact of zeta potential of early cement hydration phases on superplasticizer adsorption," *Cement and concrete research*, vol. 37, no. 4, pp. 537-542, 2007.
- [8] D.L. Kantro, "Influence of water-reducing admixtures on properties of cement paste—a miniature slump test," *Cement, Concrete and Aggregates*, vol. 2, no. 2, pp. 95-102, 1980.
- [9] S. Srinivasan, S.A. Barbhuiya, D. Charan, S.P. Pandey, "Characterising cement–superplasticiser interaction using zeta potential measurements," *Construction and Building Materials*, vol. 24, no. 12, pp. 2517-2521, 2010.

- [10] ASTM C230 / C230M-14, "Standard Specification for Flow Table for Use in Tests of Hydraulic Cement," *ASTM International*, West Conshohocken, PA, 2014.
- [11] P.C. Aïtein, C. Jolicoeur, & J.G. MacGregor, "A look at certain characteristics of superplasticizers and their use in the industry," *Concrete international*, vol. 16, no. 15, pp. 45-52, 1994.
- [12] L. Ferrari, J. Kaufmann, F. Winnefeld, J. Plank, "Interaction of cement model systems with superplasticizers investigated by atomic force microscopy, zeta potential, and adsorption measurements," *Journal of colloid and interface science*, vol. 347, no. 1, pp. 15-24, 2010.
- [13] B. Salopek, D. Krasic, S. Filipovic, "Measurement and application of zeta-potential," *Rudarsko-geolosko-naftni zbornik*, vol. 4, no. 1, pp. 147-151, 1992.
- [14] A. Uçar, "Effect of surface properties on fluorite flotation," PhD Thesis, Osmangazi University Institute of Science, Eskişehir, Turkey, pp. 11-22, 1995.
- [15] A. Uçar, "Colloid and surface chemistry," *Lecture notes*, pp. 138-155, 2004.
- [16] D.J. Shaw, *Introduction to colloid and surface chemistry*, Butterworths, London. pp. 231, 1970.
- [17] M.C. Fuerstenau, J.D. Miller, M.C. Kuhn, *Chemistry of Flotation, Society of Mining Engineers of the American Institute of Mining, Metallurgical and Petroleum Engineers. Inc*, New York, pp. 177, 1985.
- [18] D.N. Fuerstnau, S. Chander, "Thermodynamics of flotation, advances in mineral processing," *In Arbiter Symposium*, pp. 121-136, 1985.
- [19] J.M.W. Mackenzie, "Zeta potential studies on mineral processing measurement techniques and applications," *Mineral Science and Engineering*, vol. 3, no. 3, pp. 25-43, 1971.
- [20] A. Uçar, Y. Kocak, A. Dorum, "Çimento sektöründe zeta potansiyeli," *Engineering Sciences*, vol. 5, no. 3, pp. 308-318, 2010.
- [21] N. Marriaga-Cabrales, F. Machuca-Martínez, "Fundamentals of electrocoagulation," *PeraltaHernández, JM, Rodrigo-Rodrigo, MA & Martínez-Huitle, CA In: Evaluation of Electrochemical Reactors as a New Way to Environmental Protection*, Kerala: Research Signpost, pp. 1-16, 2014.
- [22] B. Ersoy, T. Kavas, S. Dikmen, E. Akbulut, A. Olgun, F.M. Kavas, "Saf C3S Fazının Zamana Bağlı Zeta Potansiyel (ZP) Değişimi İle Hidratasyonu Davranışı (Prizlenme) Arasındaki İlişki," *Afyon Kocatepe Üniversitesi Fen Ve Mühendislik Bilimleri Dergisi*, vol. 14, no. 3, pp.479-488, 2014.
- [23] K. Yıldız, A. Dorum, Y. Koçak, "Pomza Zeolit ve Cem I Çimentosunun Minerolojik Moleküler Elektrokinetik ve Termal Uyumunun Yüksek Dayanımlı Betona Etkisinin Araştırılması," *Gazi Üniversitesi Mühendislik Mimarlık Fakültesi Dergisi*, vol. 25, no. 4, pp. 867-879, 2010.
- [24] M. Löbbus, J. Sonnfeld, H.P. van Leeuwen, W. Vogelsberger, J. Lyklema, "An improved method for calculating zeta-potentials from measurements of the electrokinetic sonic amplitude," *Journal of Colloid and interface Science*, vol. 229, no. 1, pp. 174-183, 2000.
- [25] TS EN 197-1, "Cement—Part 1: Composition, Specifications and Conformity Criteria for Common Cements," *Turkish Standard Institution*, Ankara, 2012.

[26] M. Gökçe, O. Şimşek, The effect of calcite and blast furnace slag on the rheology properties of self-compacting concrete in meso and macro scales. *Revista de la construcción*, vol. 20, no. 1, pp. 190-204, 2021.